Int. J. Morphol.,
44(3):994-999, 2026.

Insulin-Induced Toxicity Promotes Morphological and Biochemical Alterations in Cardiomyocytes

La Toxicidad Inducida por Insulina Promueve Alteraciones Morfológicas y Bioquímicas en los Cardiomiocitos

Leila Smail[1]; Sihem Berdja[1]; Saliha Boumaza[1]; Samia Neggazi[1]; Nadjiba Hamlat[1] & Souhila Aouichat Bouguerra[1]

SMAIL, L.; BERDJA, S.; BOUMAZA, S.; NEGGAZI, S.; HAMLAT, N. & BOUGUERRA, S. A. Insulininduced toxicity promotes morphological and biochemical alterations in cardiomyocytes. *Int. J. Morphol., 44(3)*:994-999, 2026.

SUMMARY: Diabetic cardiomyopathy, commonly associated with insulin resistance and hyperinsulinemia, is characterized by impaired myocardial insulin signaling, mitochondrial dysfunction, endoplasmic reticulum stress, disrupted calcium homeostasis, altered coronary microcirculation, and maladaptive immune responses. These pathophysiological alterations contribute to oxidative stress, myocardial fibrosis, hypertrophy, diastolic dysfunction, and eventually systolic heart failure. In this study, cardiomyocytes of *Rattus norvegicus* were exposed to a high insulin concentration (10 IU/mL) for 6 hours. Inflammatory and oxidative stress markers were assessed, and cellular morphology was examined using May-Grünwald-Giemsa staining. High-dose insulin exposure significantly increased oxidative stress and inflammation, while reducing cell viability under hyperinsulinemic conditions. These findings indicate that insulin toxicity induces oxidative stress via reactive oxygen species generation and triggers inflammatory responses, highlighting its potential role in the pathogenesis of type 2 diabetes-associated cardiomyopathy.

KEY WORDS: Type 2 diabetes; Insulin; Apoptosis; Inflammation; Oxidative stress.

INTRODUCTION

Cardiovascular diseases remain a leading cause of diabetes-associated morbidity and mortality, and diabetic cardiomyopathy (DCM) has emerged as a distinct cardiac complication, independent of coronary artery disease and hypertension (Jia *et al*., 2018). DCM is characterized by structural and functional alterations of the myocardium, including extracellular matrix accumulation, apoptosis, diastolic dysfunction, and metabolic abnormalities (Bugger & Abel, 2014). In patients with type 2 diabetes, these pathological changes are further accelerated by comorbid conditions such as hyperlipidemia and hypertension, ultimately leading to left ventricular hypertrophy, myocardial fibrosis, and progression to heart failure (Fang *et al*., 2004). The pathophysiology of DCM involves multiple interconnected mechanisms. Mitochondrial oxidative stress plays a central role by promoting excessive generation of reactive oxygen species (ROS), thereby driving contractile dysfunction and fibrotic remodeling (Bugger & Abel, 2014). Cardiac insulin resistance disrupts energy metabolism and exacerbates myocardial dysfunction (Jia *et al*., 2018). In parallel, chronic inflammation mediated by NF-κB, TNF-α, and MCP-1 significantly contributes to myocardial remodeling and disease progression (Frati *et al*., 2017). The interplay between oxidative stress and inflammatory pathways establishes a vicious cycle that worsens both metabolic and structural abnormalities (Fang *et al*., 2004). Furthermore, advanced glycation end products and cardiac lipotoxicity have been implicated as amplifiers of myocardial injury in diabetes (Frati *et al*., 2017). Despite these advances, the mechanistic links between oxidative stress, insulin resistance, and inflammation in DCM remain incompletely understood. Therefore, the aim of the present study was to characterize experimental DCM by investigating oxidative stress, insulin resistance, inflammatory mediators (TNF-a, MCP-1, NF-kB), and myocardial morphological alterations.

MATERIAL AND METHOD

Animals. Male Wistar rats were housed in a temperature-controlled room and provided water and food ad libitum. They were acclimatized to laboratory condition for one week prior to the experiments.

[1] Laboratory of Physiology of Organisms, Team of Cellular and Molecular Physiopathology, Faculty of Biological Sciences, University of Sciences and Technology, Houari Boumedienne, (USTHB) Algiers, Algeria.

Received: 2025-11-02 Accepted: 2026-04-08

Diet. The composition of the standard laboratory diet proposed by National Livestock Feed Office (ONAB) https://www.onabnutrition.dz . A rat's daily intake is 20 g equivalent of 9 calories.

Culture of cardiomyocyte. Cardiomyocytes were cultured according to previously described methods (Aouichat Bouguerra *et al*., 2001). Briefly, explants were obtained from the ventricles of adult male Wistar rats (*Rattus norvegicus*, 250-280 g). The tissue was enzymatically dissociated by 0.1% trypsin (Gibco, USA) and subsequently incubated in Dulbecco's Modified Eagle Medium (DMEM; Gibco, USA) supplemented with 20% fetal calf serum (Sigma, USA), 1% antibiotics (streptomycin 50 mg/mL and penicillin 50 U/mL; Sigma, USA), and 1.2% L-glutamine (Sigma, USA). Cultures were maintained at 37 °C in a humidified incubator with 5% CO_2 until confluence. At confluence, cardiomyocytes were detached with 0.1% trypsin (Gibco, USA) and subcultured. Cells from the fifth passage were used in all experiments to ensure stability and reproducibility. For experimental procedures, cardiomyocytes were seeded in 12-well plates and randomly allocated into two groups:

- Control group – cells maintained in standard culture medium.
- Insulin group – cells exposed to insulin (Novo Nordisk, Denmark; 10 U/mL) for 6 h.

Study of the proliferation. At the fifth passage, cardiomyocytes were detached by trypsinization, resuspended, and seeded for 48 h under standard culture conditions. After this period, cells were exposed to insulin (Novo Nordisk, Denmark; 10 U/mL) for 6 h. Following treatment, cells were harvested again by trypsinization and stained with 0.2 % Trypan Blue solution (Sigma, USA). Cell viability and proliferation were assessed on a 100 mL suspension using a Malassez hemocytometer.

Morphological study. The suspended cells were incubated for 48 h and subsequently exposed to insulin (10 IU/mL) for 6 h. Following incubation, the culture medium was removed, and the cells were washed with phosphate-buffered saline (PBS, 1X; Gibco). The cells were then fixed with aqueous Bouin's solution and stained using May–Grünwald–Giemsa (MGG; Fluka, V/V). Morphological observations were carried out with an inverted microscope (Zeiss).

Redox Status Markers

1. **Determination of Malondialdehyde (MDA).** Lipid peroxidation was assessed by quantifying malondialdehyde (MDA) levels using the thiobarbituric acid reactive substances (TBARS) assay, according to the method of Ohkawa *et al*., (1979). Briefly, samples were centrifuged at 10,000 g for 20 min at 4 °C in 0.2 M phosphate buffer (Na?HPO?/NaH?PO?, pH 6.5). The supernatant was mixed with 10% (w/v) trichloroacetic acid (TCA) and incubated with thiobarbituric acid (TBA; Sigma, USA) to allow the formation of a pink MDA–TBA adduct. The absorbance of the complex was measured spectrophotometrically at 532 nm. MDA concentrations were expressed as nmol/mg protein.

2. **Determination of protein carbonyls.** Protein carbonyl content was determined according to the method described by Reznick and Packer, using 2,4-dinitrophenylhydrazine (DNPH; Sigma, USA) with spectrophotometric quantification. Briefly, 4 mL of 10 mM DNPH prepared in 2.5 M HCl was added to 1 mL of cellular lysate from control and insulin-treated cardiomyocytes (10 IU/mL). For blank samples, 4 mL of 2.5 M HCl was added instead of DNPH. The mixtures were incubated at room temperature in the dark for 1 h with gentle mixing every 15 min. Proteins were precipitated with 5 mL of 20 % (w/v) trichloroacetic acid (TCA), and the pellets were washed once with 10 % TCA and three times with ethanol/ethyl acetate (1:1, v/v) to remove unreacted DNPH and lipid contaminants. After centrifugation (6000 g, 5 min), the final protein pellets were dissolved in 1 mL of 6 M guanidine-HCl solution. Absorbance was measured at 370 nm, and the carbonyl content was expressed as nanomoles of carbonyl groups per milligram of protein, using a molar extinction coefficient of 22,000 M^{-1} cm^{-1}.

3. **Determination of Advanced Protein Oxidation Products (AOPP).** Advanced protein oxidation products (AOPP) were determined spectrophotometrically according to the modified method of Witko-Sarsat *et al*. Briefly, cellular lysates from control and insulin-treated (10 U/μL) groups were incubated with 1.16 M potassium iodide. After 2 min, 200 μL of acetic acid was added, and the absorbance was immediately measured at 340 nm. AOPP levels were expressed as micromoles of chloramine-T equivalents.

4. **Superoxide Dismutase Activity Determination.** Superoxide dismutase (SOD) activity was determined following the method of Dhindsa *et al*. (1980), which relies on the spectrophotometric measurement of inhibition in the photochemical reduction of nitroblue tetrazolium (NBT) at 560 nm. The reaction mixture consisted of 50 mM potassium phosphate buffer (pH 7.8), 13 mM methionine, 75 mM NBT, 0.1 mM EDTA,

4 mM riboflavin, and the appropriate volume of enzyme extract. The reaction was initiated by the addition of riboflavin, and the tubes were exposed to two 15 W fluorescent lamps for 15 min. A complete reaction mixture without enzyme extract, which yielded maximal color, was used as the control, whereas a non-irradiated reaction mixture served as the blank. One unit of SOD activity was defined as the amount of enzyme required to inhibit NBT reduction by 50%, as monitored at 560 nm.

5. **Catalase (CAT) Activity Determination.** Catalase (CAT) activity was determined spectrophotometrically according to the method of Claiborne (1985), by monitoring the rate of hydrogen peroxide (H_2O_2) decomposition at 240 nm. The reaction mixture consisted of 50 mM potassium phosphate buffer (pH 7.0), 0.33 mM H_2O_2, and an appropriate volume of enzyme extract. The decrease in absorbance was recorded for 1–3 min at 25 °C. CAT activity was expressed as units per milligram of protein, where one unit was defined as the amount of enzyme required to decompose 1 μmol of H_2O_2 per minute under the assay conditions.

Inflammatory markers

1. **Determination of Nitrogen Monoxide (NO).** The measured concentration represents the sum of nitrite and nitrate. The conversion of nitrate to nitrite is based on a cadmium reduction reaction described in (Grand, 2001).

2. **Tumor Necrosis Factor-a (TNF-α), Monocyte Chemoattractant Protein-1 (MCP-1), and Nuclear Factor Kappa B (NF-κB)**. levels were determined using an immunoenzymatic assay. The optical density was measured at 450 nm using an ELISA microplate reader (BioTek Instruments, USA).

Insulin Resistance Markers

1. **Insulin Receptor Substrate-1 (IRS-1) and Protein Kinase B (AKT)** concentrations were quantified using Invitrogen ELISA kits, following the manufacturer's instructions.

Statistical analysis

Data were analyzed using one-way ANOVA in GraphPad Prism version 8.0 (GraphPad Software, USA). Results are expressed as mean ± standard deviation (SD), and statistical significance was set at $P \leq 0.05$.

Ethical approval.

The present study was approved by the institutional Animal Care Committee of the National Administration of the Algerian Higher Education and Scientific Research (DGRSDT; https://www.dgrsdt.dz) and Use Committee of the University of Bab Ezzouar (Algiers, Algeria; Permit number for the present research project: (F00220110048) and has been achieved according to the Executive Decree no.10 n90 completing the executive Decree no. 04- 82 of the Algerian government, establishing the terms and modalities of animal welfare in animal facilities.

RESULTS

Proliferation study. Our in vitro findings revealed a highly significant reduction in cell viability following exposure to 10 U/mL of insulin (32.82 % vs. 94.60 % in the control group). In parallel, cell mortality markedly increased under this experimental condition (67.18 % vs. 5.40 % in controls) (Fig. 1).

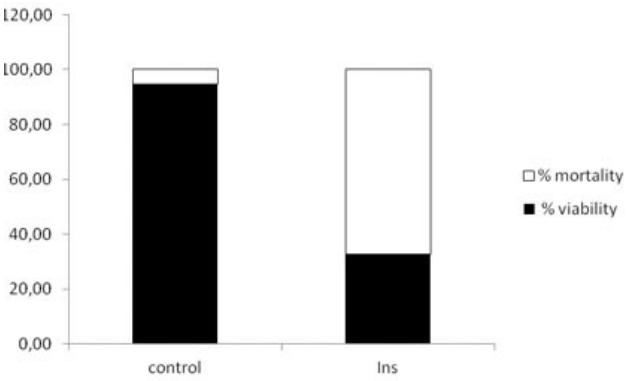

Fig. 1. Effect of high-dose insulin exposure on the viability of Rattus norvegicus cardiomyocytes. Control: untreated cardiomyocytes; Ins: cardiomyocytes exposed to 10 U/mL of insulin for 6 h.

Morphological study. Observation under the inverted microscope revealed that cells exposed to 10 U/mL of insulin for 6 h exhibited marked cytoplasmic vacuolization, cellular hypertrophy, and signs of oncosis. Moreover, a pronounced chromatin hypercondensation indicative of apoptosis was observed in these treated cells (Fig. 2B), compared with the control group (Fig. 2A).

Insulin resistance and inflammatory markers. The elevation of phosphorylated IRS1 at Ser312, accompanied by a reduction in phosphorylated AKT at Ser473, in cardiomyocytes exposed to insulin, indicates the development of insulin resistance and inflammation, as evidenced by the increased levels of TNF-a, NO, and MCP-1 (Table I).

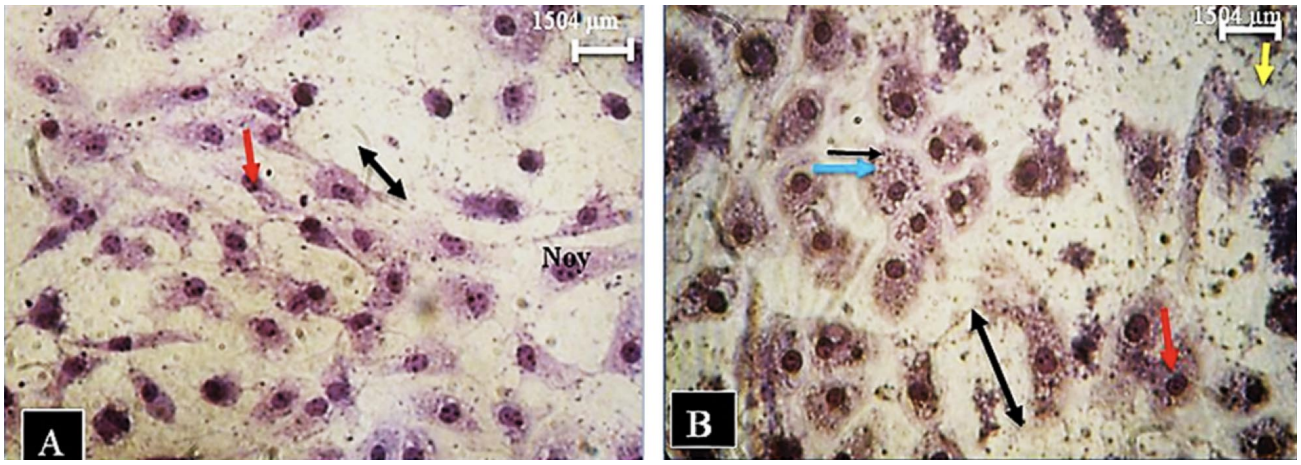

Fig. 2. May–Grünwald–Giemsa (MGG) staining of cardiomyocytes incubated in the absence or presence of insulin (10 U/mL) for 6 h. (A) Control cardiomyocytes showing normal morphology with regular size (⟷) , intact nuclei, and homogeneous cytoplasm. (B) Cardiomyocytes exposed to 10 U/mL insulin for 6 h exhibited marked cytoplasmic vacuolation (→), cell hypertrophy (→), cytoplasmic granules (→), an increased number of nucleoli (→), and membrane budding features indicative of apoptosis and oncosis. Cells were fixed in aqueous Bouin's solution, stained with MGG, and observed under an inverted microscope (Zeiss, ×200).

Table I. Effects of high-dose insulin (10 U/mL) exposure on insulin resistance, inflammatory, and apoptotic markers in Rattus norvegicus cardiomyocytes.

Markers	Control	Insulin (10 U/mL)	Pathophysiological Category
IRS1 p[S312] (units/10^6 cells)	2.17 ± 0.52	6.73 ± 3.12****	Insulin resistance
AKT p[S473] (units/10^6 cells)	4.73 ± 0.13	2.01 ± 0.13****	Insulin resistance
TNF-α (pg/10^6 cells)	12.68 ± 1.74	51.83 ± 4.47****	Inflammatory
MCP-1 (pg/10^6 cells)	71.77 ± 8.95	118.81 ± 16.03****	Inflammatory
NO (pmol/10^6 cells)	14.26 ± 0.57	26.31 ± 4.22****	Inflammatory
Cytochrome c (ng/10^6 cells)	1.02 ± 0.08	1.97 ± 0.13****	Apoptotic

Data presentation: Values are expressed as mean ± SEM (n = 3). ****p < 0.0001 (Insulin-treated vs. Control group). IRS1 p[S312], Insulin Receptor Substrate-1 (phosphorylated at Ser 312); AKT p[S473], Protein Kinase B (phosphorylated at Ser 473); TNF-α, Tumor Necrosis Factor-α; MCP-1, Monocyte Chemotactic Protein-1; NO, Nitric Oxide; Cyt c, Cytochrome c.

Redox status markers Exposure of cells to insulin-induced stress resulted in a highly significant increase in MDA, AOPP, and protein carbonyl contents ($p < 0.0001$), along with a marked decrease in catalase activity and a concomitant increase in SOD activity ($p < 0.0001$) (Table II).

Table II. Redox status markers of cardiomyocytes exposed to insulin (10 U/mL).

Markers	Control	Insulin (10 U/mL)
MDA (µmol/10^6 cells)	1.08 ± 0.05	2.39 ± 0.22****
AAOP (pmol/10^6 cells)	0.24 ± 0.02	0.58 ± 0.08****
PC (pmol/10^6 cells)	1.77 ± 0.21	17.32 ± 0.48****
SOD (µU/mg/10^6 cells)	1.38 ± 0.00	5.37 ± 0.00****
CAT (U/mg/10^6 cells)	0.10 ± 0.00	0.05 ± 0.00****

Data presentation: Values are expressed as mean ± SEM (n = 3). ****p < 0.0001 (Insulin-treated vs. Control group). MDA, Malondialdehyde; AAOP, Advanced Protein Oxidation Products; PC, Protein Carbonyls; SOD, Superoxide Dismutase; CAT, Catalase.

DISCUSSION

Our investigation provided valuable insights into the pathophysiological mechanisms by which supraphysiological insulin exposure affects cardiomyocytes of *Rattus norvegicus*. Exposure to 10 U/mL insulin resulted in a marked decline in cellular proliferation and a concomitant increase in cell death compared with control cells, suggesting that high insulin concentrations trigger cytotoxic and pro-apoptotic cascades. Similar findings were reported by Saltiel and Kahn, 2001, who demonstrated that hyperinsulinemia impairs b-cell viability under hyperglycemic stress. Such outcomes are consistent with the well-established concept that chronic insulin exposure promotes insulin and cellular stress, leading to apoptotic or necrotic outcomes. Microscopic examination revealed cytoplasmic vacuolization,

hypertrophy, and chromatin condensation, indicative of apoptosis and oncosis. These observations support the findings of Tischler *et al*., (1997) and Chi *et al*., (2000), who observed insulin-induced cytotoxicity and apoptosis in muscle and embryonic cells, respectively. The overexpression of cytochrome c (Cyt c) in insulin-treated cardiomyocytes confirms mitochondrial involvement in the apoptotic process, which is consistent with previous studies showing that mitochondrial dysfunction and oxidative stress are central mediators of insulin-induced cell death (Mailloux, 2018). At the molecular level, increased phosphorylation of IRS1 at Ser312, accompanied by reduced AKT phosphorylation (Ser473), indicates an insulin-resistant phenotype. This impairment in insulin signaling may result from TNF-α–mediated serine phosphorylation of IRS1 via the JNK and IKKb pathways, as previously described by Hotamisligil *et al*., (1996). This proinflammatory cytokine cascade inhibits the normal tyrosine phosphorylation of IRS1, thus attenuating downstream PI3K/AKT signaling and reducing glucose uptake (Samuel & Shulman, 2012). The increased levels of TNF-α, MCP-1, and NO observed in our model further confirm a state of metabolic inflammation, in line with reports showing that hyperinsulinemia enhances oxidative and inflammatory signaling in cardiac tissue (Bugger & Abel, 2014). Oxidative stress was another prominent outcome in our study. Exposure to 10 IU/ml insulin led to a significant increase in malondialdehyde (MDA), advanced oxidation protein products (AOPP), and protein carbonyls, reflecting lipid and protein oxidation. These findings align with the results of (Guo *et al*. 2014; Pieri *et al.*, 2023) , who documented a similar rise in oxidative stress markers under hyperinsulinemic or diabetic conditions. Interestingly, SOD activity was elevated, possibly as a compensatory response to increased ROS production, while catalase activity declined, indicating a redox imbalance. Such an imbalance may promote peroxynitrite formation, protein nitration, and irreversible oxidative injury (Monnier *et al*., 2005; Alhumaydhi *et al.*, 2025). Overall, our findings suggest that sustained insulin exposure induces a dual mechanism involving oxidative stress and inflammation, which synergistically contribute to insulin resistance and cardiomyocyte apoptosis. This phenomenon could mimic the cardiometabolic disturbances observed in type 2 diabetes, where hyperinsulinemia coexists with elevated oxidative and inflammatory stress. The activation of stress-sensitive kinases (JNK, p38 MAPK) and inhibition of the PI3K/AKT pathway may represent a molecular link between insulin toxicity and cardiac remodeling (Snel *et al*., 2012; Shulman, 2014; Trouwborst *et al*., 2018). Thus, targeting oxidative and inflammatory pathways might provide novel therapeutic strategies to mitigate insulin-induced cardiac dysfunction.

CONCLUSION

In conclusion, the present study demonstrated that exposure to high concentrations of insulin induces in vitro insulin toxicity in *Rattus norvegicus* cardiomyocytes. This toxicity is associated with pronounced inflammatory and oxidative disturbances, which may contribute to the development of cardiovascular complications commonly observed in type 2 diabetes.

SMAIL, L.; BERDJA, S.; BOUMAZA, S.; NEGGAZI, S.; HAMLAT, N. & BOUGUERRA, S. A. La toxicidad inducida por insulina promueve alteraciones morfológicas y bioquímicas en los cardiomiocitos. *Int. J. Morphol., 44(3)*:994-999, 2026.

RESUMEN: La cardiomiopatía diabética, comúnmente asociada con resistencia a la insulina e hiperinsulinemia, se caracteriza por una alteración en la señalización de la insulina miocárdica, disfunción mitocondrial, estrés del retículo endoplasmático, alteración de la homeostasis del calcio, alteración de la microcirculación coronaria y respuestas inmunitarias desadaptativas. Estas alteraciones fisiopatológicas contribuyen al estrés oxidativo, la fibrosis miocárdica, la hipertrofia, la disfunción diastólica y, finalmente, la insuficiencia cardíaca sistólica. En este estudio, se expusieron cardiomiocitos de *Rattus norvegicus* a una alta concentración de insulina (10 UI/mL) durante 6 horas. Se evaluaron marcadores de inflamación y estrés oxidativo, y se examinó la morfología celular mediante tinción de May-Grünwald-Giemsa. La exposición a altas dosis de insulina aumentó significativamente el estrés oxidativo y la inflamación, a la vez que redujo la viabilidad celular en condiciones hiperinsulinémicas. Estos hallazgos indican que la toxicidad de la insulina induce estrés oxidativo mediante la generación de especies reactivas de oxígeno y desencadena respuestas inflamatorias, lo que subraya su posible papel en la patogénesis de la cardiomiopatía asociada a la diabetes tipo 2.

PALABRAS CLAVE: Diabetes tipo 2; Insulina; Apoptosis; Inflamación; Estrés oxidativo.

REFERENCES

Alhumaydhi, F. A.; Younus, H. & Khan, M. A. Catalase functions and glycation: Their central roles in oxidative stress, metabolic disorders, and neurodegeneration. *Catalysts, 15(9)*:817, 2025.

Aouichat-Bouguerra, S.; Bourdillon, M. C.; Dahmani, Y. & Bekkhoucha, F. Non insulin dependent diabetes in sand rat (Psammomys obesus) and production of collagen in cultured aortic smooth muscle cells. Influence of insulin. *Int. J. Exp. Diabetes Res., 2(1)*:37-46, 2001.

Bugger, H. & Abel, E. D. Molecular mechanisms of diabetic cardiomyopathy. *Diabetologia, 57*:660-71, 2014.

Chi, M. M. Y.; Schlein, A. L. & Moley, K. H. High insulin-like growth factor 1 (IGF-1) and insulin concentrations trigger apoptosis in the mouse blastocyst via down-regulation of the IGF-1 receptor. *Endocrinology, 141(12)*:4784-92, 2000.

Claiborne, A. *Catalase activity*. In: Greenwald, R. A. (Ed.). CRC Handbook of Methods for Oxygen Radical Research. Boca Raton, CRC Press, 1985.

Dhindsa, R. S.; Plumb-Dhindsa, P. & Thorpe, T. A. Leaf senescence: Correlated with increased levels of membrane permeability and lipid peroxidation, and decreased levels of superoxide dismutase and catalase. *J. Exp. Bot., 32(1)*:93-101, 1981.

Fang, Z. Y.; Prins, J. & Marwick, T. Diabetic cardiomyopathy: Evidence, mechanisms, and therapeutic implications. *Endocr. Rev., 25(4)*:543-67, 2004.

Frati, G.; Schirone, L.; Chimenti, I.; Yee, D.; Biondi-Zoccai, G.; Volpe, M. & Sciarretta, S. Overview of the inflammatory signalling mechanisms linking diabetic cardiomyopathy to myocardial inflammation. *Cardiovasc. Res., 113(4)*:378-84, 2017.

Grand, F.; Guitton, J. & Goudable, J. Optimisation of the measurement of nitrite and nitrate in serum by the Griess reaction. Ann. Biol. Clin. (Paris)., 59(5):559-65, 2001.

Guo, S. Insulin signaling, resistance, and the metabolic syndrome: Insights from mouse models into disease mechanisms. *J. Endocrinol., 220(2)*:T1-T23, 2014.

Hotamisligil, G. S.; Peraldi, P.; Budavari, A.; Ellis, R.; White, M. F. & Spiegelman, B. M. IRS-1-mediated inhibition of insulin receptor tyrosine kinase activity in TNF-a- and obesity-induced insulin resistance. *Science, 271(5249)*:665-8, 1996.

Trouwborst, I.; Bowser, S. M.; Goossens, G. H. & Blaak, E. E. Ectopic fat accumulation in distinct insulin resistant phenotypes: Targets for personalized nutritional interventions. *Nutrients, 10(1)*:77, 2018.

Jia, G.; Hill, M. A. & Sowers, J. R. Diabetic cardiomyopathy: An update of mechanisms contributing to this clinical entity. *Circ. Res., 122(4)*:624-38, 2018.

Mailloux, R. J.; Young, A.; O'Brien, M. & Gill, R. M. Simultaneous measurement of superoxide/hydrogen peroxide and NADH production by flavin-containing mitochondrial dehydrogenases. *J. Vis. Exp., (132)*:e56975, 2018.

Monnier, L.; Mas, E.; Ginet, C.; Michel, F.; Villon, L.; Cristol, J. P. & Colette, C. Activation of oxidative stress by acute glucose fluctuations compared with sustained chronic hyperglycemia in patients with type 2 diabetes. *JAMA, 295(14)*:1681-7, 2006.

Snel, M.; Jonker, J. T.; Schoones, J.; Lamb, H.; de Roos, A.; Pijl, H.; Smit, J. W. A.; Meinders, A. E. & Jazet, I. M. Ectopic fat and insulin resistance: Pathophysiology and effect of diet and lifestyle interventions. *Int. J. Mol. Sci., 13(5)*:1706-47, 2012.

Ohkawa, H.; Ohishi, N. & Yagi, K. Assay for lipid peroxides in animal tissues by thiobarbituric acid reaction. Anal. Biochem., 95:351-8, 1979.

Pieri, B. L. S.; Rodrigues, M. S.; Farias, H. R.; Silveira, G. B.; Ribeiro, V. S. G. C.; Silveira, P. C. L. & de Souza, C. T. Role of oxidative stress on insulin resistance in diet-induced obesity mice. *Int. J. Mol. Sci., 24(15)*:12088, 2023.

Prieto, P.; Pineda, M. & Aguilar, M. Spectrophotometric quantitation of antioxidant capacity through the formation of a phosphomolybdenum complex: Specific application to the determination of vitamin E. *Anal. Biochem., 269(2)*:337-41, 1999.

Reznick, A. Z. & Packer, L. Oxidative damage to proteins: Spectrophotometric method for carbonyl assay. Methods Enzymol., 233:357-63, 1994.

Saltiel, A. R. & Kahn, C. R. Insulin signalling and the regulation of glucose and lipid metabolism. *Nature, 414(6865)*:799-806, 2001.

Samuel, V. T. & Shulman, G. I. Mechanisms for insulin resistance: Common threads and missing links. *Cell, 148(5)*:852-71, 2012.

Shulman, G. I. Ectopic fat in insulin resistance, dyslipidemia, and cardiometabolic disease. *N. Engl. J. Med., 371(12)*:1131-41, 2014.

Tischler, M. E.; Satarug, S.; Aannestad, A.; Muñoz, K. A. & Henriksen, E. J. Insulin attenuates atrophy of unweighted soleus muscle by amplified inhibition of protein degradation. *Metabolism, 46(6)*:673-9, 1997.

Witko-Sarsat, V.; Friedlander, M.; Nguyen-Khoa, T.; Capeillère-Blandin, C.; Nguyen, A. T.; Zingraff, J.; Jungers, P. & Descamps-Latscha, B. Advanced oxidation protein products as a novel marker of oxidative stress in uremia. *Kidney Int., 49(5)*:1304-13, 1996.

Corresponding author:
Dr. Leila Smail
Faculty of Biological Sciences
University of Sciences and Technology
Houari Boumedienne
(USTHB) Algiers
ALGERIA

E-mail: leila84.smail@gmail.com